www.sciencemag.org/cgi/content/full/344/6187/1023/DC1

Supplementary Materials for

Composition of isolated synaptic boutons reveals the amounts of vesicle trafficking proteins

Benjamin G. Wilhelm, Sunit Mandad, Sven Truckenbrodt, Katharina Kröhnert, Christina Schäfer, Burkhard Rammner, Seong Joo Koo, Gala A. Claßen, Michael Krauss, Volker Haucke, Henning Urlaub, Silvio O. Rizzoli

*To whom correspondence should be addressed. E-mail: srizzol@gwdg.de

Published 30 May 2014, *Science* **344**, 1023 (2014)
DOI: 10.1126/science.1252884

This PDF file includes:

Other Supplementary Material for this manuscript includes the following:
(available at www.sciencemag.org/cgi/content/full/344/6187/1023/DC1)

Materials and Methods

Purification and characterization of synaptosomes

Synaptosomes were purified from adult Wistar rats (five to six weeks old) as previously described (*35, 6*). The cortex and cerebellum were homogenized in ice-cold sucrose buffer (320 mM Sucrose, 5 mM HEPES, pH 7.4) with a glass-Teflon homogenizer. The homogenate was subjected to two differential centrifugations (3,000 g for 4 min and 14,000 g for 12 min) before applying one gradient centrifugation (6%, 9% and 13% Ficoll in sucrose buffer at 86,000 g for 35 min). The latter resulted in separation into four different fractions. The fraction at the interface of the 9% and 13% Ficoll contained the majority of synaptosomes and was therefore used for all experiments performed in this study. Immediately after purification, the synaptosomes were snap frozen in liquid nitrogen and stored at -80 °C until used in biochemistry experiments.

The total amount of particles in the synaptosome preparation was determined by immobilizing them on BSA-coated coverslips by centrifugation (2,900 g for 50 min), and imaging their membranes in FM 1-43 labeling, using a fluorescence microscope (IX71, Olympus, Tokio, Japan) equipped with a 100x 1.4 NA oil immersion objective (UPlanSApo, Olympus) and with a F-View II CCD camera (12 bit; 6.54 µm pixel size). FM 1-43 fluorescence was detected using a 480/40 HQ excitation filter, a 505 LP Q beamsplitter, and a 527/30 HQ emission filter (Chroma Technology Corporation, Bellows Falls, VT). All visible particles were counted and extrapolated to the total surface of the cover-slip in order to obtain the number of particles present in a defined quantity of the synaptosome preparation. To correct for the bias introduced by the incomplete immobilization of particles onto coverslips, samples of the supernatant taken before and after centrifugation were immunoblotted for two reference proteins (syntaxin 1 and VAMP 2; see description of immunoblots in the protein quantification section). The relative amount of protein left in the supernatant after centrifugation was used to determine the efficiency of the spin down, which was applied as a correction factor to the counted number of particles.

Cell cultures and neuromuscular junctions

Primary hippocampal neuronal cultures were obtained from newborn (P1 – P3) Wistar rats as previously described (*36*). They were used between 15 – 20 days in culture. The *levator auris longus* muscle of adult wild-type mice (CD-1, B6/N and B6/J) was dissected exactly as described (*21*). Animals were handled in accordance with the regulations of the University of Göttingen and of the State Niedersachsen (Landesamt für Verbraucherschutz, LAVES, Braunschweig, Germany).

Electron microscopy and reconstruction of synaptosomes

Directly after purification, synaptosomes were processed and embedded for electron microscopy. Fixation was performed in phosphate buffered saline (PBS, 150 mM NaCl, 20 mM Na_2HPO_4, pH 7.4) containing 2.5% glutaraldehyde,

followed by quenching in PBS containing 100 mM NH_4Cl. After thoroughly washing off remaining fixative with PBS, the samples were osmicated in PBS containing 1% OsO_4, washed again and embedded in low melt Agarose (Sigma-Aldrich, St. Louis, MO). After a dehydration series in ethanol, the Agarose blocks were embedded in Epon and polymerized. Samples were cut into approximately 70-nm-thin sections using a Leica microtome (EM UC 6, Leica Microsystems, Wetzlar, Germany). Imaging was performed using a JEOL JEM1011 electron microscope (JEOL GmbH, Munich, Germany) equipped with an Orius SC1000A 1 camera (Gatan Inc., Pleasanton, CA), at 4008x2672 pixels.

For reconstructing entire synaptosomes, serial thin sections were imaged and aligned manually in Photoshop (Adobe Systems, San Jose, CA). The different components of the synaptosomes were selected individually in each frame, and the synaptosomes were reconstructed as described (see for example (*22*)).

The identity of the particles in the synaptosome preparation was determined using electron micrographs of the samples (detailed descriptions of the procedures involved in electron microscopy are provided in the next section). All visible particles in the images were manually selected by experienced observers and assigned to the following specific categories: synaptosomes, postsynaptic fragments, mitochondria, myelin, myelin fragments, vacuoles, endosome-like organelles, free SVs. Using a custom-written Matlab routine (The Mathworks, Inc., Natick, MA), each particle was compared to the surrounding particle-free background. The particle area that was denser than the background was measured and was used to determine the percentage of the preparation made up by the respective particle. This procedure avoided the over-representation of large, empty vacuoles or of broken myelin membranes.

Immunofluorescence-based spin down assay

3 µg of synaptosomes (total protein) were centrifuged onto 18 mm glass cover-slips for 50 min at 2900 g and 4°C. Prior to this the cover-slips were incubated in PBS with 5% BSA at 37°C, overnight, and were coated with 0.2 µm TetraSpeck™ beads (Invitrogen, 1 ml of $1:10^6$ diluted beads in PBS, centrifuged for 50 min at 2900 g, 4°C). The beads were used to align the images taken from the synaptosomes, since the beads are visible in all channels. Afterwards, the synaptosomes were fixed for 10 min on ice and 45 min at room temperature, with PBS containing 4% PFA (Paraformaldehyde) followed by quenching in PBS + 100 mM NH 4 Cl for 30 min at room temperature. Subsequently, after a brief wash in PBS, the samples were blocked and permeabilized for 30 min in PBS + 0.1% Triton X100 + 5% BSA followed by a 1 h incubation with primary antibodies in the same solution. The synaptosomes were incubated with antibodies against Synaptotagmin 1 for labeling SVs. After the antibody incubation the samples were washed briefly in PBS. Secondary antibodies were applied under the same conditions as the primary antibody. To remove excess antibodies the samples were washed consecutively with high salt and regular PBS prior to imaging.

Directly after labeling, the samples were imaged in a 1:20 dilution of a saturated solution of 1-(4-Trimethylammoniumphenyl)-6-Phenyl-1,3,5-Hexatriene p-Toluenesulfonate (TMA-DPH) in ddH_2O. TMA-DPH is an amphiphilic dye, which emits fluorescence around 440 nm rendering it an ideal candidate for labeling membranes in parallel to the immunostaining. Hence, TMA-DPH labels all particles of the samples, thus serving as a positive labeling control for this assay. Imaging was performed at the same Olympus set-up as described above, using 100x magnification. As mentioned above, the TetraSpeck^{TM} beads were fluorescent in all four channels. Alexa488 images (where only beads were visible) were used as a reference to align the images during analysis.

Image analysis was performed using custom written Matlab routines. The position of the beads was used to align the images obtained in the different channels. The amount of total particles was derived by counting the number of TMA-DPH labeled spots while the amount of synaptosomes was derived from the fraction of TMA-DPH labeled which were positively labeled for Synaptotagmin 1. Free synaptic vesicles, which would have complicated the analysis, were too dim to discern in either of the fluorescence channels, and were also not abundant in the preparation (Fig. S1B).

Protein quantification

Proteins were separated by electrophoresis using 10% denaturing Tris/Tricin SDS polyacrylamide gels in a discontinuous buffer system (anode buffer containing 200 mM TRIS at pH 8.9 and cathode buffer containing 100 mM TRIS, 100 mM Tricin, 1% SDS, pH 8.25), as described in the past (*37*). Prior to loading, samples were boiled at 95 °C in sample buffer (50 mM TRIS, 4% SDS, 0.01% Serva Blue G, 12% Glycerol, 2% β-Mercaptoethanol, pH 6.8). After separation the proteins were blotted onto a nitrocellulose membrane (0.2 µm, Perkin Elmer, Waltham, MA) in a wet blotting tank (Biorad, Hercules, CA) at 4 °C in transfer buffer (200 mM Glycin, 25 mM TRIS, 20% Methanol, 0.04% SDS). Next, membranes were blocked and immunolabeled with primary antibodies in blocking buffer (PBS + 5% low fat milk powder + 0.1% Tween-20). The primary antibodies used for the detection of the different proteins can be found on the data sheet for the respective proteins in Fig. S5. The detection of primary antibodies was performed using secondary antibodies coupled to an infrared dye (IRDye 800 CW, LI-COR Biosciences, Lincoln, NE); imaging was performed using the LI-COR Odyssey imaging system at a high resolution and highest sensitivity. Custom-written Matlab routines were used to measure the band intensity corrected for local background (see (*38*)). Fetal calf serum (FCS) was added to the purified proteins for the quantification of presynaptic proteins, in amounts matching the total protein concentration in the synaptosome samples. See Supplemental Experimental Procedures for more details.

Several proteins were treated differently in order to separate and blot efficiently: AP-2 (mu2), clathrin heavy chain, clathrin light chain, Doc2, endophilin,

Munc13a, Munc18a, vATPase (A1) and VDAC were blotted without the addition of FCS to avoid masking the signal by components of the serum. SV2 and vATPase were not boiled prior to separation to avoid protein aggregation. CALM was blotted on PVDF membranes (Millipore, Billerica, MA).

The laboratories of the following collaborators kindly presented us with some of the purified proteins used to determine the amount of protein in synaptosomes: Reinhard Jahn (Max-Planck Institute for Biophysical Chemistry, Göttingen, Germany; α-SNAP, Munc13a, Munc18a, NSF, SNAP 25, Synaptotagmin 1, Syntaxin 1, Syntaxin 6, Syntaxin 7, Syntaxin 13, Syntaxin 16, VAMP 2, VAMP 4 and Vti1A), Christian Griesinger (Max-Planck Institute for Biophysical Chemistry, Göttingen, Germany; α-Synuclein), Beat Schwaller (University of Fribourg, Switzerland; Calbindin, Calretinin and Paralbumin), and Aurelien Roux (University of Geneva, Switzerland; Dynamin 1). GST-rat AP180 (aa 1-297), GST-full length rat CALM, full length human SEPT5 in pGEX4T-1, GST-human SGIP1 (aa 1-220) in pGEX5T-1, and His_6-PIPKIγ (aa 451-668) were transformed into *E. coli* BL21-Codon Plus™ (DE)-RP competent cells (Stratagene, Böblingen, Germany). Fusion proteins were expressed at 25°C for PIPK Iγ, septin 5, AP 180 and CALM and 16°C for SGIP1 overnight and purified using His-Select® Nickel Affinity Gel (Sigma) or GST Bind® resin (Novagen, Darmstadt, Germany), respectively, following the manufacturer's instructions. Recombinant clathrin heavy chain and ITSN were expressed and purified as described previously (*39, 40*). All other purified proteins were purchased from Novus Biologicals (Littleton, CO).

Protein concentrations for the synaptosomes and for the purified proteins were determined using a bicinchoninic acid assay (BCA, Invitrogen, Carlsbad, CA), measuring the absorbance with a spectrophotometer (Nanodrop ND1000, Peqlab, Erlangen, Germany). The concentrations of most purified proteins were further confirmed using Coomassie and silver stainings of protein gels, following standard protocols.

Correction factors for the potential loss of soluble proteins during purification were obtained by comparing relative amounts of protein in synaptosomes with those in the same synapses from brain slices obtained from rats of similar age. Synaptosomes (see detailed immunostaining procedure below) and brain slices were labeled and imaged in parallel for the soluble protein of interest and for the transmembrane synaptic vesicle protein synaptophysin. Cortical brain slices were obtained as recently described (*41*). The slices were blocked with PBS containing 10% BSA and incubated with the primary antibodies in PBS containing 2% BSA and 0.1% Triton X-100. Afterwards, samples were washed thoroughly and incubated with secondary antibodies in PBS containing 2% BSA. Prior to imaging, slices were washed in PBS and embedded in Mowiöl. Both synaptosomes and slices were imaged with confocal resolution using the Leica TCS SP5 STED microscope described below. The two samples were imaged in parallel using identical imaging settings (zoom, laser intensity, gain and pinhole

size). All the primary antibodies used for this assay are listed under the respective proteins in Fig. S5. For detection, secondary antibodies conjugated to Cy3 (synaptophysin) and to Cy5 (protein of interest) were used (both from Dianova, Hamburg, Germany). Images were analyzed using custom-written Matlab routines. The synaptophysin signal served as a marker for presynaptic sites, and its intensity was used as a reference for the intensity of the synapse. The ratios of protein-of-interest intensity over synaptophysin intensity obtained from the two samples (synaptosomes and slices) were then used to calculate a correction factor for the respective protein. Similar ratios indicated no significant changes after synaptosome purification. Lower rations in synaptosomes were indicative of a loss of protein of interest.

Sample preparation for LC-MSMS

Four different samples were used for label-free absolute quantification as previously described (*12*). *i*) 10.6 µg of Universal Proteome Standard (UPS2, Sigma-Aldrich), ii) 1 µg each of the purified recombinant proteins used in the Western Blot analysis (see above), iii) 10 µg of *E. coli* lysate, and finally iv) 10 µg of rat brain synaptosomes (four biological replicates).All four samples were hydrolyzed with trypsin (Promega Corp., Mannheim, Germany; enzyme:protein ratio of 1:50) in the presence of RapiGest^{TM} SF Surfactant (Waters, Milford, MA) according to the protocols provided by the manufacturer. Digestion time for UPS2, purified recombinant proteins, and E. coli lysate was 16 h, 37 °C. Digestion time for synaptosomal proteins was set to 8h, 12h, 16h, 24h, and 48h in order to evaluate the most intense iBAQ values for absolute quantification (see below). Peptide mixtures were desalted using C18 StageTips (*42*). Samples were dried under vacuum and stored at -20°C.

LC-MS/MS

Each sample was analyzed in three technical replicates by LC-MSMS. For LC-MS analysis, the peptides derived from each sample were dissolved in 5% (v/v) acetonitrile and 1% (v/v) formic acid. In each case the equivalent of 1 µg starting protein sample was injected for LC-MSMS analysis. LC-MSMS was carried using the following conditions: Peptides were loaded on an Agilent 1100 nano-flow LC system (Agilent Technologies, Böblingen, Germany) equipped with an in-house packed C18 trap column (1.5 cm, 360 µm outer diameter, 150 µm inner diameter, Reprosil-Pur 120 Å, 5 µm, C18-AQ, Dr. Maisch, Ammerbuch-Entringen, Germany) at flow rate 10 µl/min and washed for 5 min with Buffer A (0.1% formic acid). Peptide separation was done on an in-house-packed C18 column (15 cm, 360 µm outer diameter, 75 µm inner diameter, Reprosil-Pur 120 Å, 5 µm, C18-AQ, Dr. Maisch) at a flow rate of 300 nl/min with a gradient from 5-38% of Buffer B (95% acetonitrile, 0.1% formic acid) for 90 min. Eluting peptides were analyzed on-line obn a LTQ-Orbitrap Velos hybrid mass spectrometer (Thermo Electron) operating in a Data Dependent acquisition mode where the 15 most intense ions in the MS scan (m/z range from 400 to 1200, resolution set to 30,000 at m/z 400) were selected for fragmentation by collision induced dissociation (CID) and analyzed in the ion trap. Automatic gain control target was set at 30,000 and 10^6

for Ion Trap and FTMS respectively. Sequenced precursors were put on an exclusion list for 30 sec. The lock mass option (m/z 445.120025) was used for internal calibration (*43*).

Mass spectrometry data analysis

Data were analyzed using MaxQuant (version 1.3.0.5) (*13*) with Andromeda search engine (*14*). Data were searched against a SwissProt rat protein database (March 2013; containing 7842 reviewed entries) and in case of UPS2 against a UPS2 protein database (48 entries). Mass deviation was set to 6 ppm (MS) and 10 ppm (MS/MS). Oxidation of methionine and carbamidomethylation of cysteines were set as variable and fixed modifications, respectively. For enzyme specify (trypsin) no proline restriction and up to two missed cleavages were set. False discovery rate (FDR) was set at 1%. The iBAQ option in Andromeda search engine was enabled for quantification (using the log10 fit option in MaxQuant).

Quantification of synaptosomal proteins by iBAQ

To obtain iBAQ values of proteins present in UPS2, 1 µg of *E. coli* tryptic digest was mixed with 1 µg of the trypsinized UPS2 standard and analyzed by LC-MS/MS as above in three technical replicates with a total amount of 1 ug on column. Similarly, six fold dilutions of 1 µg of recombinant proteins (used for quantitative western blots) were also spiked with 1 µg of E. coli lysate all separately and analyzed by LC-MS/MS. The obtained iBAQ values (*12*) were plotted against the known amounts of the proteins in the UPS2. Similarly, the six fold dilutions of known amounts of individual recombinant synaptosomal protein were plotted against their iBAQ values. The slopes were calculated for UPS2 and recombinant synaptosomal proteins by taking the mean values of the technical replicates. The absolute amounts of proteins present in synaptosome were calculated by linear regression using the slopes of UPS2, alternatively the slopes of individual recombinant synaptosomal proteins to correlate the absolute amounts of same proteins in synaptosome. The absolute amounts of the four biological replicates of synaptosomes were averaged. The moles of individual proteins were multiplied first with Avogadro's number to calculate the number of molecules and then were divided by the average number of synaptosomes present per µg, to obtain the copy numbers per synaptosomes. The quantified proteins were assigned to various categories based on DAVID Functional Annotation Bioinformatics Microarray Analysis (*44, 45*). The contaminants were removed from the protein list.

Protein localization

All three preparations (synaptosomes, neuronal cultures and mouse neuromuscular junction, NMJ) were stained in parallel for the protein of interest and for an active zone and a vesicle marker. Bassoon was used as an active zone marker for synaptosomes and neuronal cultures (using primary antibodies from Stressgene, ADI-VAM-PS003-D or Synaptic Systems, 141 002). In the NMJ the postsynaptic acetylcholine receptors were labeled with bungarotoxin coupled

to tetramethylrhodamin (Sigma-Aldrich, T0195). In all preparations, the vesicle cluster was detected using antibodies targeted to synaptophysin (Synaptic Systems, 101 004). The antibodies used for the detection of the protein of interest are listed in Fig. S5. Secondary antibodies coupled to Cy2 (for bassoon in synaptosomes and cultures, and for synaptophysin in the NMJs; Dianova), to Cy3 (for synaptophysin in synaptosomes and cultures; Dianova) and to Atto647N (for the protein of interest; Synaptic Systems, Sigma or Rockland) were used.

Synaptosomes centrifuged onto BSA-coated coverslips were fixed in PBS containing 4% PFA and quenched with PBS containing 100 mM NH_4Cl. Blocking and antibody incubation (primary and secondary) were performed in PBS + 2.5% BSA + 0.1% Triton X-100. After being repeatedly washed in PBS and in PBS + 350 mM NaCl (high-salt PBS), the synaptosomes were embedded in Mowiöl.

Primary hippocampal cultures were fixed with PBS + 4% PFA and quenched with PBS containing 100 mM NH_4Cl. Incubation with primary and secondary antibodies was performed in PBS + 1.5% BSA + 0.1% Triton X-100. After thoroughly washing the samples with PBS and high-salt PBS, they were subjected to a TDE (2,2'-thiodiethanol, Sigma (*46*), dilution series (30 – 100% in ddH_2O) and finally embedded in 100% TDE (see also (*31*)).

The *levator auris longus* muscles were dissected in standard mouse saline as described (*36*). The muscles were fixed in PBS + 4% PFA and quenched in PBS with 100 mM NH_4Cl. Blocking was performed using PBS + 2.5% BSA + 0.5% Triton X-100. Several antibodies demanded stronger blocking conditions to ensure labeling specificity (BACE, Epsin 1, Munc13a, Syndapin, PIPK Iγ, Septin 5, SGIP1, SNAP 23, SNAP 25, Synaptotagmin 2, Syntaxin 16, VAMP 2, vATPase A1). In these cases, 5% BSA and an additional 5% of Tryptone/Peptone were used. Primary antibodies were incubated in the same blocking solution, while the detergent was omitted for the secondary antibody incubation. Like the neuronal cultures, the muscles were treated with a TDE dilution series prior to being embedded in 100% TDE.

Imaging was performed using a Leica TCS SP5 STED microscope equipped with a 100x and 1.4 NA oil immersion objective (HCX PL APO CS, Leica).

Confocal imaging was performed using the 488 nm line of an Argon laser (for Cy2) and the 543 nm line of a Helium Neon laser (for Cy3 and tetramethylrhodamin). For the STED imaging of the protein of interest (Atto647N), a pulsed diode laser with 635 nm was used for excitation; depletion was achieved at 750 nm using a Spectra-Physics MaiTai tunable laser (Newport Spectra-Physics, Irvine, CA). The AOTF filter of the microscope was used to select appropriate emission intervals for the different dyes. Signal detection was performed either by a photomultiplier (confocal mode) or by an avalanche photodiode (STED mode). For display purposes, the fluorescence images were deconvolved with Huygens Essential software (Scientific Volume Imaging,

Hilversum, The Netherlands), using the inbuilt routines recommended by the company.

Image analysis was performed using custom-written Matlab routines. The center of mass of the active zone signal was determined for each synapse. The regions of interest surrounding each active zone (1 µm for synaptosomes and hippocampal synapses; 3 µm for NMJs) were aligned so that the centers of mass of the active zones overlapped. The images were then rotated to obtain the maximum overlap between the different synaptophysin images and between the images of the protein of interest. The overlap was determined measuring the Pearson's correlation coefficient between individual images; a weighted mean (between synaptophysin and protein-of-interest coefficients) was used to determine the optimal orientation of the synapses.

For synaptosomes and hippocampal cultures the antibody staining signal was sufficiently sparse to allow us to separate antibody clusters. For each antibody or antibody cluster we obtained the intensity and position. These were used to generate the average images presented in Fig. 3A,B. The spot sizes in Fig. 3A,B are indicative of the precision with which the positions of the signals could be measured in the respective experiments (tested using repeated imaging of fluorescent beads similar in size to antibody clusters). For NMJs the raw data images were directly averaged (Fig. 3C).

The parameters discussed in Fig. 3D were obtained using custom-written Matlab routines, according to the details indicated in the main text and according to previous published protocols (*22, 31, 4*). All parameters were analyzed using the relative spatial distribution of the proteins (blue panels in Fig. 3 and Fig. S5). The correlations to the active zone and to the vesicle cluster were calculated by measuring the Pearson's correlation coefficient for the images of the proteins of interest and of bassoon or synaptophysin, as markers for the active zone and the vesicle cluster, respectively. The fraction of the protein present in the active zone area was calculated as the intensity of the protein of interest in the 100-nm diameter area surrounding the center of the bassoon signal, expressed as proportion of the summed intensity of the protein of interest in the entire synapse. The fraction of the protein present in the peri-active zone area was calculated similarly, for a 50-nm diameter circle surrounding the active zone area. The enrichment of the protein in the active zone area was the ratio of the last two parameters. The fractions of the protein present in the vesicle cluster area (defined as the area covered by the synaptophysin signal), or in high intensity clusters, were calculated in a similar fashion to the fraction present in the active zone area. The coefficient of variation of the protein signal was calculated as the statistical coefficient of variation (CoV) of the spatial distribution images (blue panels in Fig. 3 and Fig. S5). The model distribution of the proteins within the synaptosome (Figure S6I) was performed based on previous published protocols (*31*).

Construction of the graphical model

The graphical model of the average presynaptic terminal was constructed using custom-written plug-ins and scripts in the 3D software Autodesk Maya (Autodesk Inc., San Rafael, CA). Information on protein structures was obtained from the Uniprot database. All the references used to model the presynaptic protein organization are listed in the reference section for each protein in Fig. S5. If available, protein data base (PDB) coordinates were used to determine the structure of a protein. In case no PDB data for an entire protein or parts of the protein existed, structural information from the following prediction servers was used to create the 3D structure manually: secondary structure (http://bioinf.cs.ucl.ac.uk/psipred/), alignment (http://web.expasy.org/sim/), coiled coil (http://toolkit.tuebingen.mpg.de/pcoils), disorder (http://mbs.cbrc.jp/poodle/poodle-s.html; http://mbs.cbrc.jp/poodle/poodle-w.html; http://mbs.cbrc.jp/poodle/poodle-l.html), transmembrane (http://www.ch.embnet.org/software/TMPRED_form.html), glycosylation (http://www.glycosciences.de/modeling/glyprot/php/main.php), domain search (http://smart.embl-heidelberg.de/index2.cgi), homologue proteins (http://web.expasy.org/blast/).

Statistics

Graphs show means ± SEM, unless otherwise indicated. The Student's t-test (unpaired) was used for establishing statistical differences (*P* values indicated in the respective figures), unless otherwise indicated.

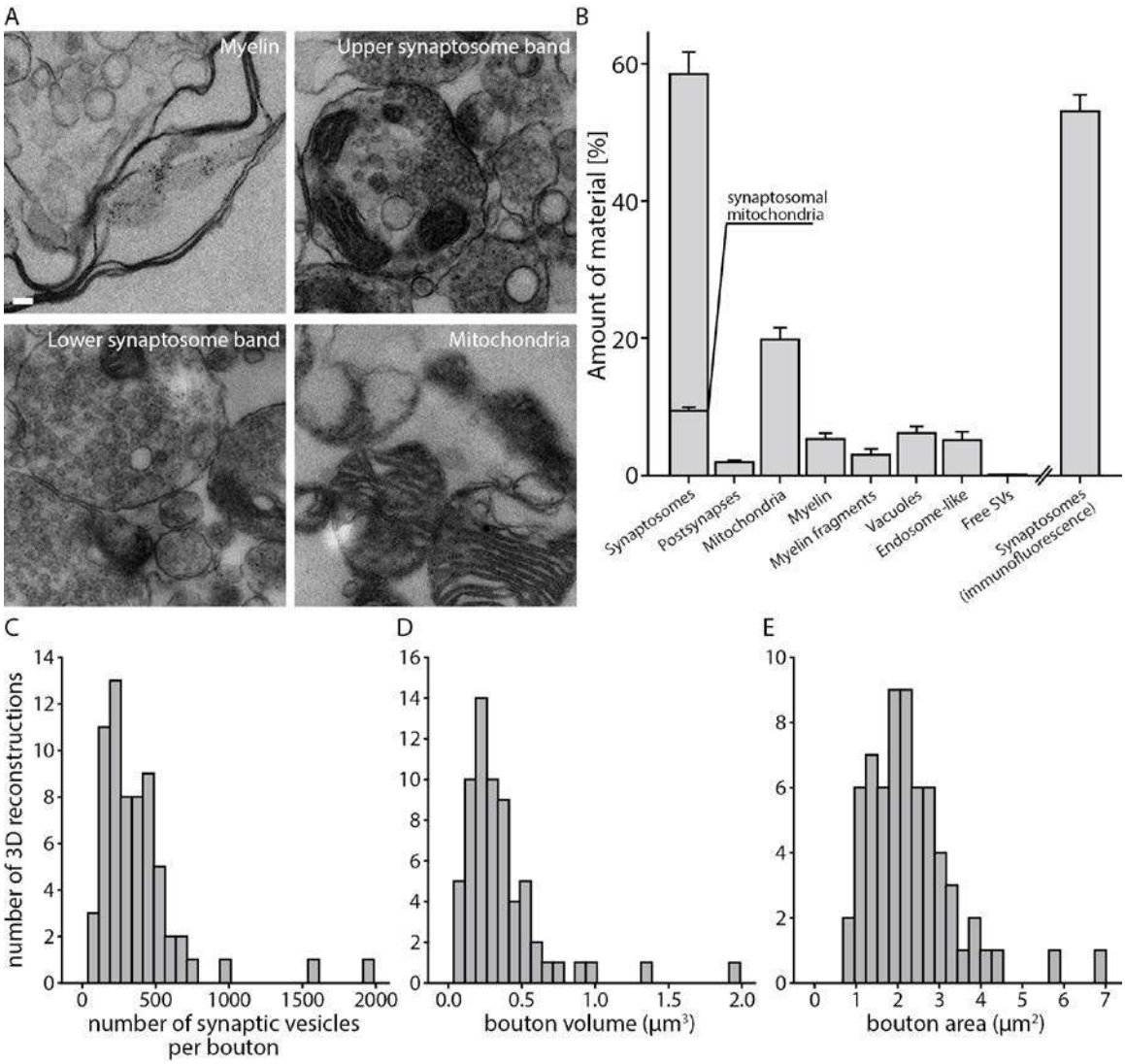

Fig. S1. Purification and composition of synaptosomes

(A) Electron micrographs of the four different fractions obtained after gradient centrifugation. Scale bar is 100 nm.

(B) Quantitative analysis of the composition of the lower synaptosome fraction by electron microscopy. Visible particles in the electron micrographs were selected and sorted into different categories. The graph represents the relative amount of the different particle categories as mean ± SEM of 4 independent preparations (see Experimental Procedures for further details). The values for mitochondria, myelin and post-synaptic elements correlate well with the values obtained from iBAQ mass spectrometry (Table S3). The last bar, to the right of the break in the X-axis, quantifies the relative amount of synaptosomes by an immunostaining approach. The particles were centrifuged onto coverslips, were immunostained for the synaptic vesicle marker synaptotagmin I, and were analyzed by imaging both synaptotagmin and a membrane marker (TMA-DPH; see Materials and Methods for details). The percentage of synaptotagmin-positive particles is indicated (mean ± SEM of 4 independent preparations; this measurement was

repeated 7-8 times for each preparation, in independent immunostaining experiments).
(C)-(E) Histograms of the number of synaptic vesicles per bouton (C), the bouton volume (D), and the bouton surface area (E) obtained from 65 synaptosome 3D-reconstructions, obtained from four independent preparations. (C) Mean ± SEM: 383.7 ± 37.9 vesicles. Median: 313 vesicles. (D) Mean ± SEM: 0.37 ± 0.04 μm^3. Median: 0.29 μm^3. (E) Mean ± SEM: 2.31 ± 0.14 μm^2. Median: 2.10 μm^2.

A

B

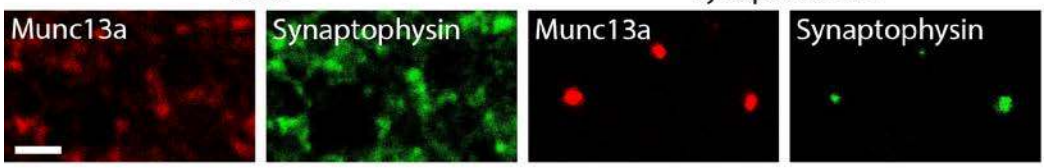

C

Protein	Ratio of relative amounts	Significance (p-value)
SNAP 25	1.01 ± 0.48	N.S.
VAMP 2	1.25 ± 0.47	N.S.
α-SNAP	1.27 ± 0.12	N.S.
α/β-Synuclein	1.11 ± 0.29	N.S.
AP 180	0.72 ± 0.22	N.S.
AP 2 (mu2)	1.09 ± 0.31	N.S.
CALM	0.47 ± 0.08	0.003
Calmodulin	1.63 ± 0.69	N.S.
Clathrin heavy chain	0.98 ± 0.31	N.S.
Clathrin light chain	0.38 ± 0.07	0.0008
Complexin 1,2	1.40 ± 0.61	N.S.
CSP	0.96 ± 0.43	N.S.
Doc2 A/B	1.03 ± 0.37	N.S.
Dynamin 1,2,3	0.96 ± 0.31	N.S.
Endophilin I,II,III	0.98 ± 0.20	N.S.
Epsin 1	0.48 ± 0.11	0.01
Hsc70	1.46 ± 0.41	N.S.
Intersectin 1	1.14 ± 0.06	N.S.
Munc13a	0.97 ± 0.45	N.S.
Munc18a	0.96 ± 0.31	N.S.
NSF	1.01 ± 0.39	N.S.
PIPK Iγ	0.65 ± 0.11	0.03
Rab3	0.61 ± 0.25	N.S.
Rab5a	1.12 ± 0.34	N.S.
Rab7a	0.78 ± 0.07	0.04
Septin 5	0.75 ± 0.29	N.S.
SGIP1	0.89 ± 0.36	N.S.
Synapsin I,II	1.68 ± 0.99	N.S.
Syndapin 1	0.95 ± 0.10	N.S.

Fig. S2. Correction for the loss of soluble proteins during purification

(A) Schematic outline of the experiment: cortical brain slices and synaptosomes were immunostained in parallel for the protein of interest (red) and for the transmembrane protein synaptophysin (green). This enabled the determination of the relative amount of the protein of interest in each preparation (protein of interest intensity relative to synaptophysin intensity). The potential loss of the protein from synaptosomes was determined by comparing the relative amounts of the protein of interest in the two preparations: a loss of the protein of interest is reflected by a lower relative intensity in synaptosomes than in slices. A correction factor was calculated if the loss was significant. The correction factor represented the ratio of the two relative amounts (synaptosomes over slices).

(B) Representative images of slices (left) and synaptosomes (right) immunostained for Munc13a (red) and synaptophysin (yellow). Scale bar is 2 µm.

(C) Table listing the amount of each protein of interest in synaptosomes, as a fraction of its amount in slice synapses (mean ± SEM of 3-5 independent experiments). Note that only five proteins (CALM, clathrin light chain, epsin 1, PIPK Iγ and Rab7) were lost in significant amounts from the synaptosomes during purification (Student's t-tests)..

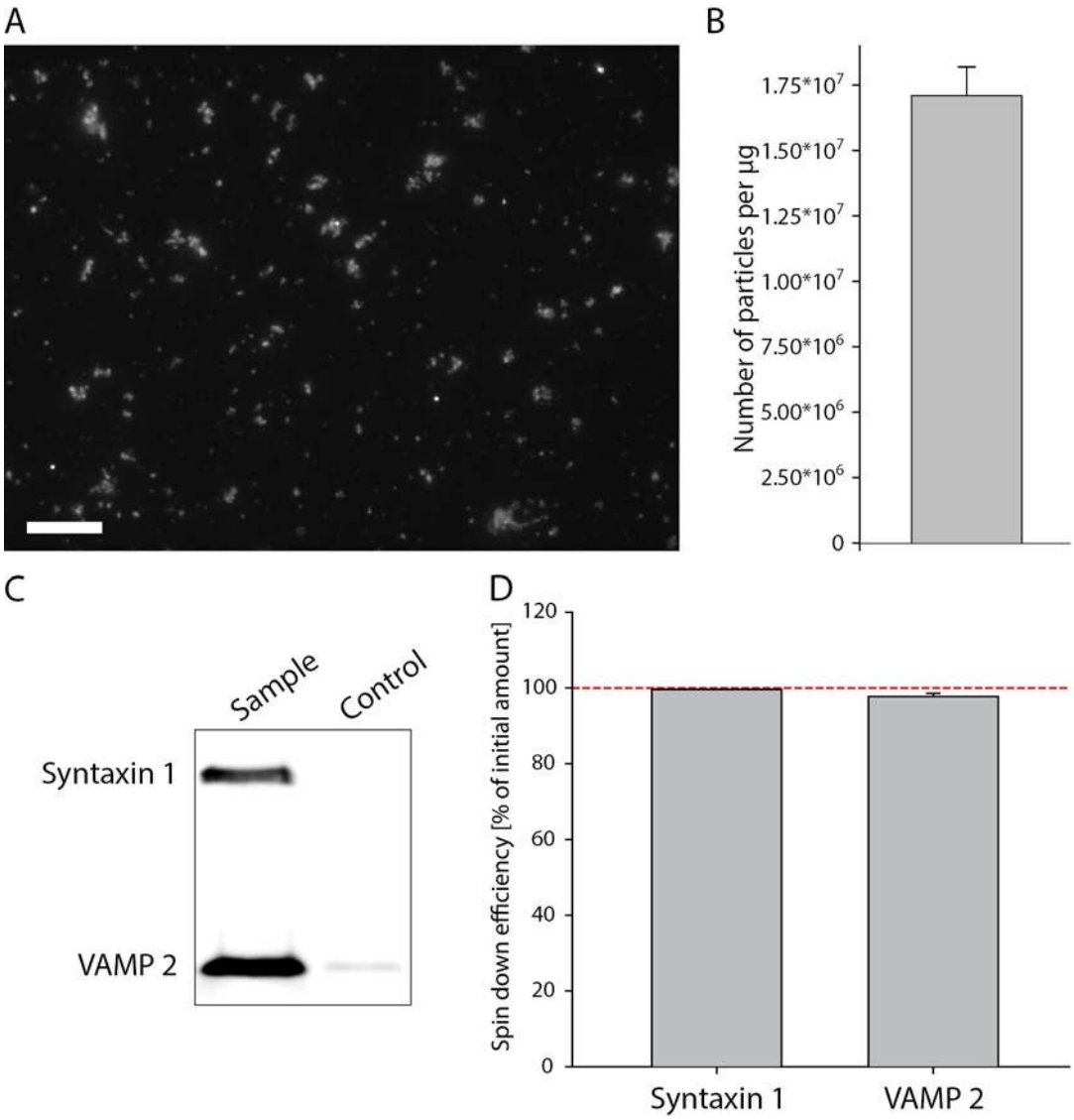

Fig. S3. Number of particles per microgram

(A) Synaptosomes were immobilized on glass coverslips and stained with membrane dye FM 1-43. Scale bar is 10 µm.

(B) Number of particles per µg, determined by counting particles stained with FM 1-43. Bar represents mean ± SEM of 7 independent experiments from 4 different preparations.

(C) Determination of the efficiency of synaptosome immobilization (via spin down) on glass coverslips. The supernatants of the coverslips before (sample) and after (control) centrifugation were immunoblotted for two prominent synaptic markers, Syntaxin 1 and VAMP 2.

(D) Spin down efficiency for the two marker proteins as fraction of the initial amount of protein cleared from the supernatant after centrifugation. Bars represent mean ± SEM of 8 independent experiments.

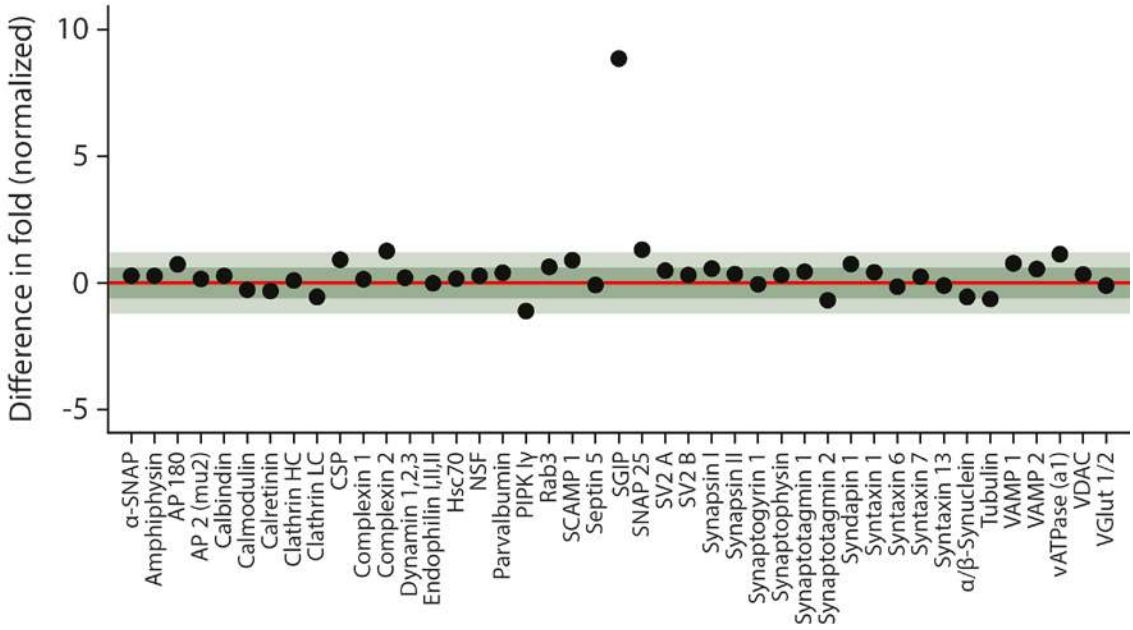

Fig. S4. Quantitative mass spectrometry confirms the protein numbers obtained by quantitative immunoblotting

The difference in fold between protein numbers determined by quantitative immunoblotting and quantitative mass spectrometry is plotted, normalized to the median internal error of the mass spectrometry measurement. The red line indicates no difference between the values obtained in quantitative immunoblotting and mass spectrometry. The dark area indicates the median internal error of the mass spectrometry measurement. The light gray area indicates the double of the median internal error.

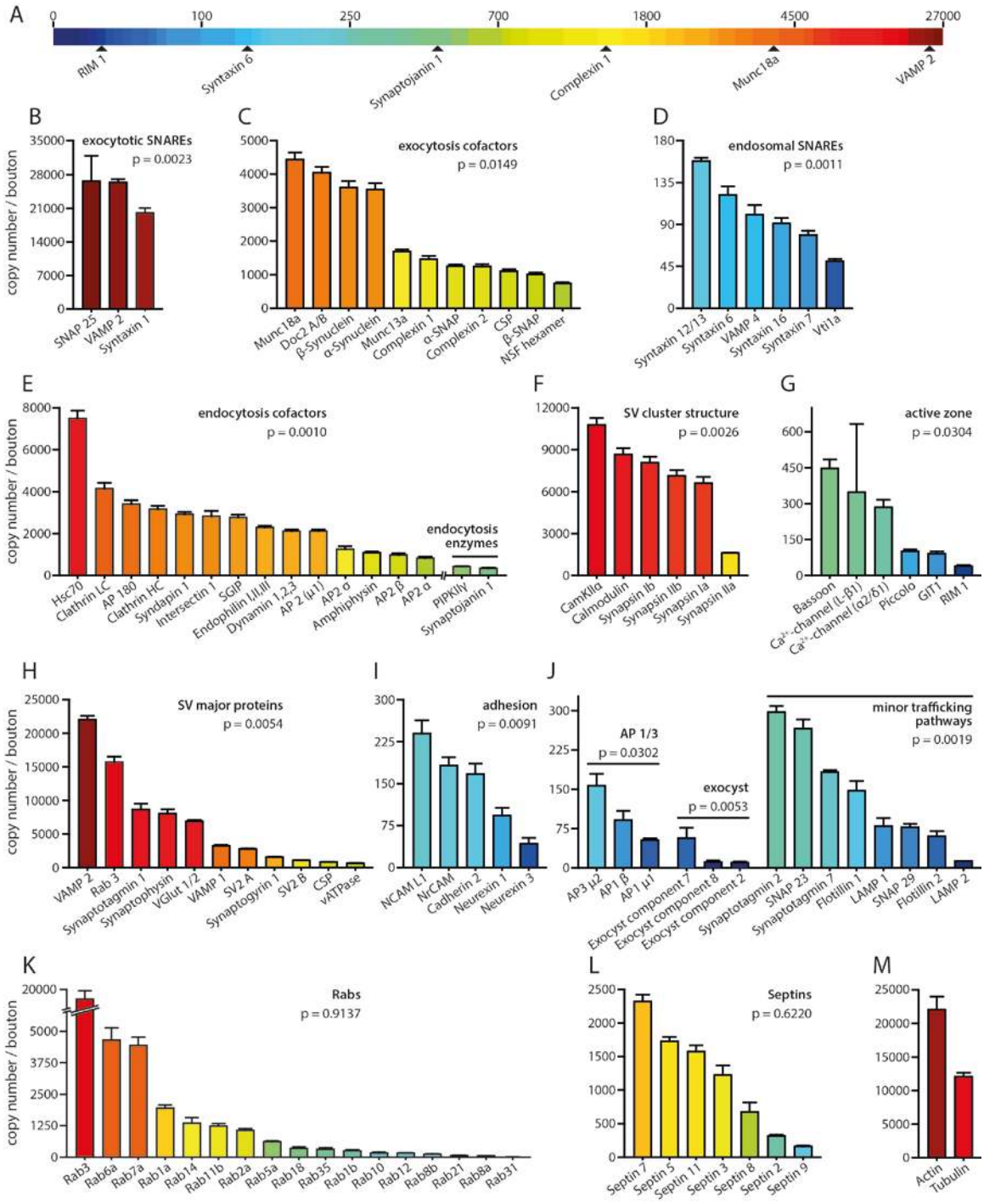

Fig. S5. Illustration of synaptic protein numbers

(A) We selected 100 different synaptic proteins, and ordered them according to abundance per synaptic bouton, from lowest (CALM) to highest (SNAP 25). Most protein numbers were obtained from quantitative Western Blotting (see Table S1 for details); several copy numbers were obtained from iBAQ mass spectrometry (see Table S2 for details).

(B-M) The copy numbers of different groups of proteins are illustrated, color coded according to the colorbar from (A). The groups are formed by proteins that participate in the same steps of synaptic activity (such as the exocytotic SNAREs, the endocytotic proteins, or the adhesion proteins), or by proteins with a similar structure (Rabs or septins). A separate group is formed by the major synaptic vesicle proteins (panel H), which appear to bind each other and/or cholesterol, and thus maintain the identity of the synaptic vesicle throughout recycling (see discussion in (*33*)). The color coding offers a visual indication of the correlation of copy numbers within the different groups. We also tested these correlations statistically by two-sample Kolmogorov-Smirnov tests. The P values are noted in each panel. Overall, the copy numbers of proteins that function together correlate significantly (for all groups analyzed). The copy numbers of structurally related proteins do not correlate. Additionally, a correlation can be detected between proteins of minor trafficking pathways (J), probably due to the fact that they are generally absent from synapses. Data are means ± SEM from 4 independent preparations.

Fig. S6 (separate file). Database of information on presynaptic proteins

The biochemistry, imaging and modeling data are presented for each protein. A detailed description of the meaning of the individual panels is presented on the first page.

The middle panels show two graphs.
Left, the relation between abundance of the protein of interest and synapse size, obtained from hippocampal cultures.The intensity of synaptophysin is shown on the x-axis, as a measure of the number of synaptic vesicles, and thus of synapse size. The intensity of the protein of interest is shown on the y-axis. Data points represent mean ± SEM. We would like to point out that the relation between the amount of synaptophysin and the amount of the protein of interest is typically linear for synaptic vesicle proteins, including VAMP2, CSP or synaptophysin itself. For many other proteins, such as the endocytotic ones, the amount of the protein of interest plateaus at high synaptophysin intensities, indicating that large synapses contain proportionally lower amounts of these proteins.

Right, the distribution of the protein of interest in relation to the active zone, again obtained from the hippocampal cultures. The x-axis indicates the distance to the center of the active zone, while the y-axis plots the average protein intensity, obtained from the protein maps from the hippocampal culture panels. Curves that fall rapidly with distance from the active zone are typical for proteins that are enriched in the active zone (such as piccolo or syntaxin 1). Conversely, proteins that are widely distributed in the synaptic volume show flatter, less steep curves (such as AP180 or NSF).

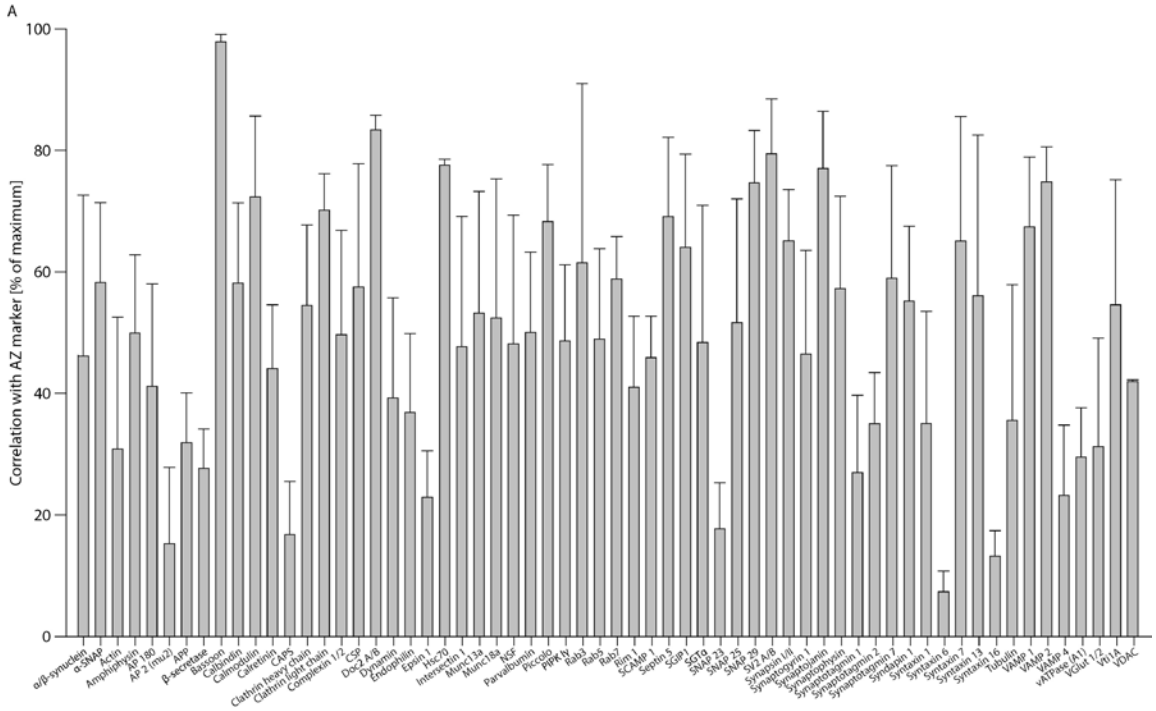
A
Correlation with AZ marker [% of maximum]
100
80
60
40
20
0
α/β-synuclein
α-SNAP
Actin
Amphiphysin
AP 180
AP 2 (mu2)
APP
β-secretase
Bassoon
Calbindin
Calmodulin
Calretinin
CAPS
Clathrin heavy chain
Clathrin light chain
Complexin 1/2
CSP
Doc2 A/B
Dynamin
Endophilin
Epsin 1
Hsc70
Intersectin 1
Munc13a
Munc18a
NGF
Parvalbumin
Piccolo
PIPK Iγ
Rab3
Rab5
Rab7
Rim 1
SCAMP 1
Septin 5
SGIP1
SGT1
SNAP 23
SNAP 25
SNAP 29
SV2 A/B
Synapsin I/II
Synaptogyrin 1
Synaptojanin
Synaptophysin
Synaptotagmin 1
Synaptotagmin 2
Synaptotagmin 7
Synbindin 1
Syntaxin 1
Syntaxin 6
Syntaxin 7
Syntaxin 13
Syntaxin 16
Tubulin
VAMP 1
VAMP 2
VAMP 4
vATPase (A1)
VGlut 1/2
V1A
VDAC

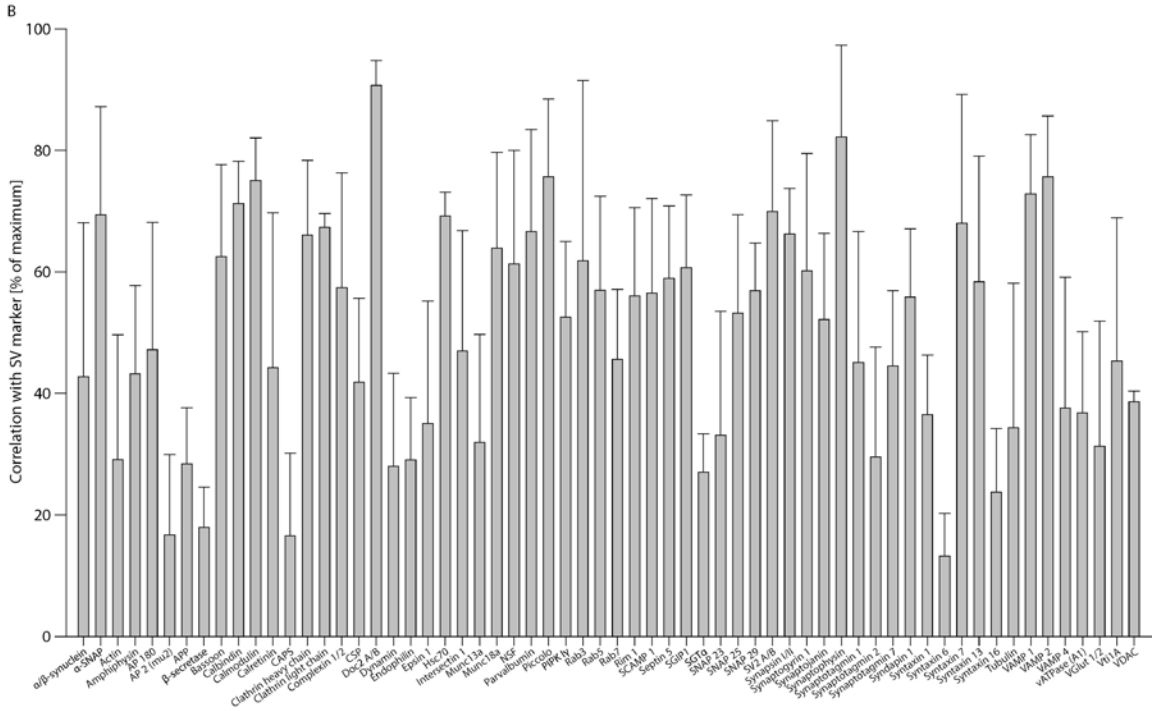
B
Correlation with SV marker [% of maximum]
100
80
60
40
20
0
α/β-synuclein
α-SNAP
Actin
Amphiphysin
AP 180
AP 2 (mu2)
APP
β-secretase
Bassoon
Calbindin
Calmodulin
Calretinin
CAPS
Clathrin heavy chain
Clathrin light chain
Complexin 1/2
CSP
Doc2 A/B
Dynamin
Endophilin
Epsin 1
Hsc70
Intersectin 1
Munc13a
Munc18a
NGF
Parvalbumin
Piccolo
PIPK Iγ
Rab3
Rab5
Rab7
Rim 1
SCAMP 1
Septin 5
SGIP1
SGT1
SNAP 23
SNAP 25
SNAP 29
SV2 A/B
Synapsin I/II
Synaptogyrin 1
Synaptojanin
Synaptophysin
Synaptotagmin 1
Synaptotagmin 2
Synaptotagmin 7
Synbindin 1
Syntaxin 1
Syntaxin 6
Syntaxin 7
Syntaxin 13
Syntaxin 16
Tubulin
VAMP 1
VAMP 2
VAMP 4
vATPase (A1)
VGlut 1/2
V1A
VDAC

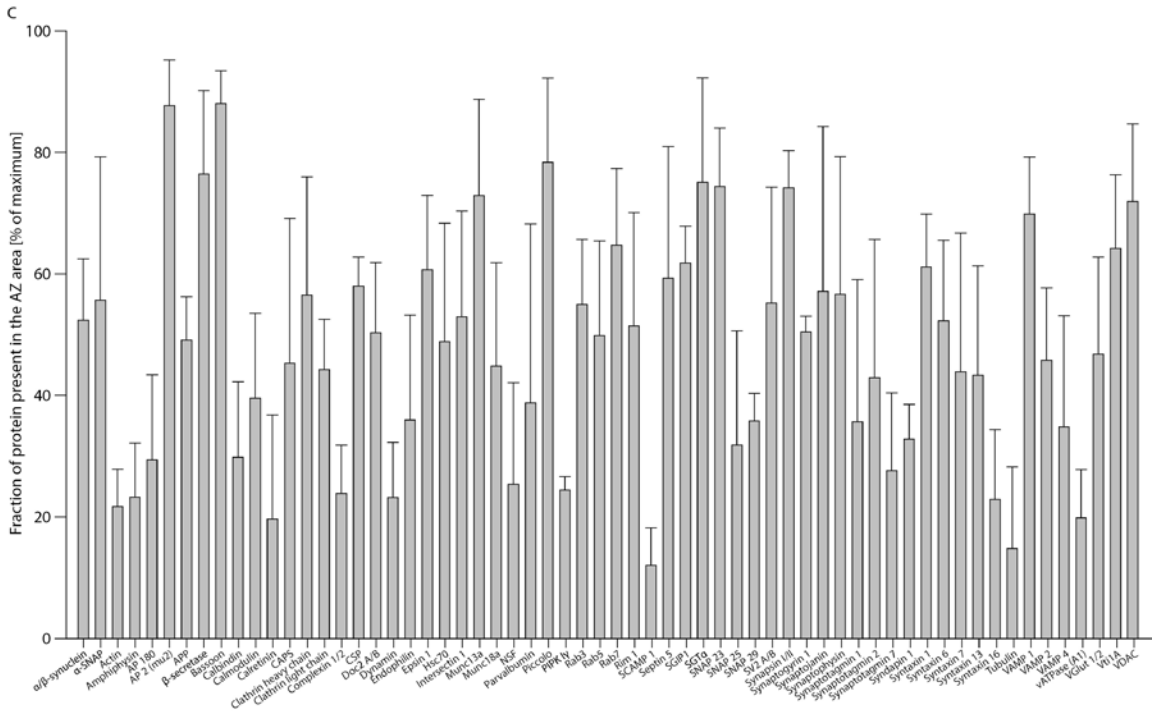
C
Fraction of protein present in the AZ area [% of maximum]
100
80
60
40
20
0
α/β-synuclein
α-SNAP
Actin
Amphiphysin
AP 180
AP 2 (mu2)
APP
β-secretase
Bassoon
Calbindin
Calmodulin
Calretinin
CAPS
Clathrin heavy chain
Clathrin light chain
Complexin 1/2
CSP
Doc2 A/B
Dynamin
Endophilin
Epsin 1
Hsc70
Intersectin 1
Munc13a
Munc18a
NGF
Parvalbumin
Piccolo
PIPK Iγ
Rab3
Rab5
Rab7
Rim 1
SCAMP 1
Septin 5
SGIP 1
SGTG
SNAP 23
SNAP 25
SNAP 29
SV2 A/B
Synapsin I/II
Synaptogyrin 1
Synaptophysin
Synaptotagmin 1
Synaptotagmin 2
Synaptotagmin 7
Synaptotagmin 12
Synaptotagmin 13
Syntaxin 1
Syntaxin 6
Syntaxin 7
Syntaxin 13
Syntaxin 16
Tubulin
VAMP 1
VAMP 2
VAMP 4
vATPase [A1]
VGlut 1/2
Vti1A
VDAC

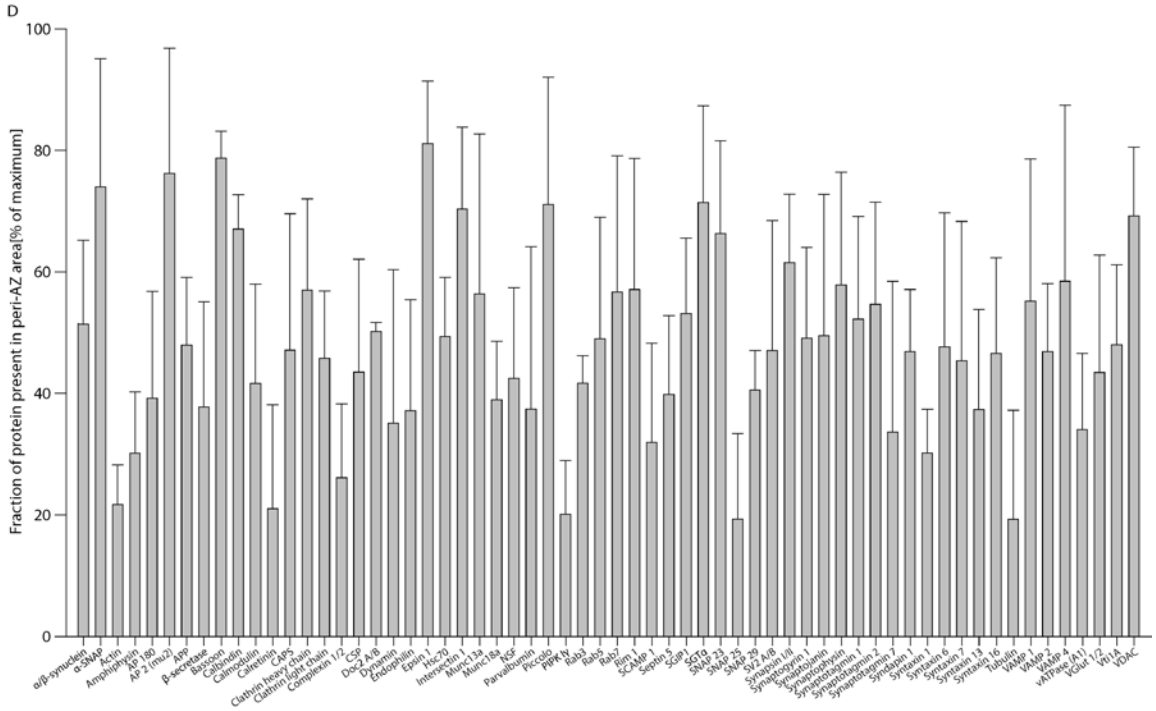
D
Fraction of protein present in peri-AZ area[% of maximum]
100
80
60
40
20
0
α/β-synuclein
α-SNAP
Actin
Amphiphysin
AP 180
AP 2 (mu2)
APP
β-secretase
Bassoon
Calbindin
Calmodulin
Calretinin
CAPS
Clathrin heavy chain
Clathrin light chain
Complexin 1/2
CSP
Doc2 A/B
Dynamin
Endophilin
Epsin 1
Hsc70
Intersectin 1
Munc13a
Munc18a
NGF
Parvalbumin
Piccolo
PIPK Iγ
Rab3
Rab5
Rab7
Rim 1
SCAMP 1
Septin 5
SGIP 1
SGTG
SNAP 23
SNAP 25
SNAP 29
SV2 A/B
Synapsin I/II
Synaptogyrin 1
Synaptophysin
Synaptotagmin 1
Synaptotagmin 2
Synaptotagmin 7
Synaptotagmin 12
Synaptotagmin 13
Syntaxin 1
Syntaxin 6
Syntaxin 7
Syntaxin 13
Syntaxin 16
Tubulin
VAMP 1
VAMP 2
VAMP 4
vATPase [A1]
VGlut 1/2
Vti1A
VDAC

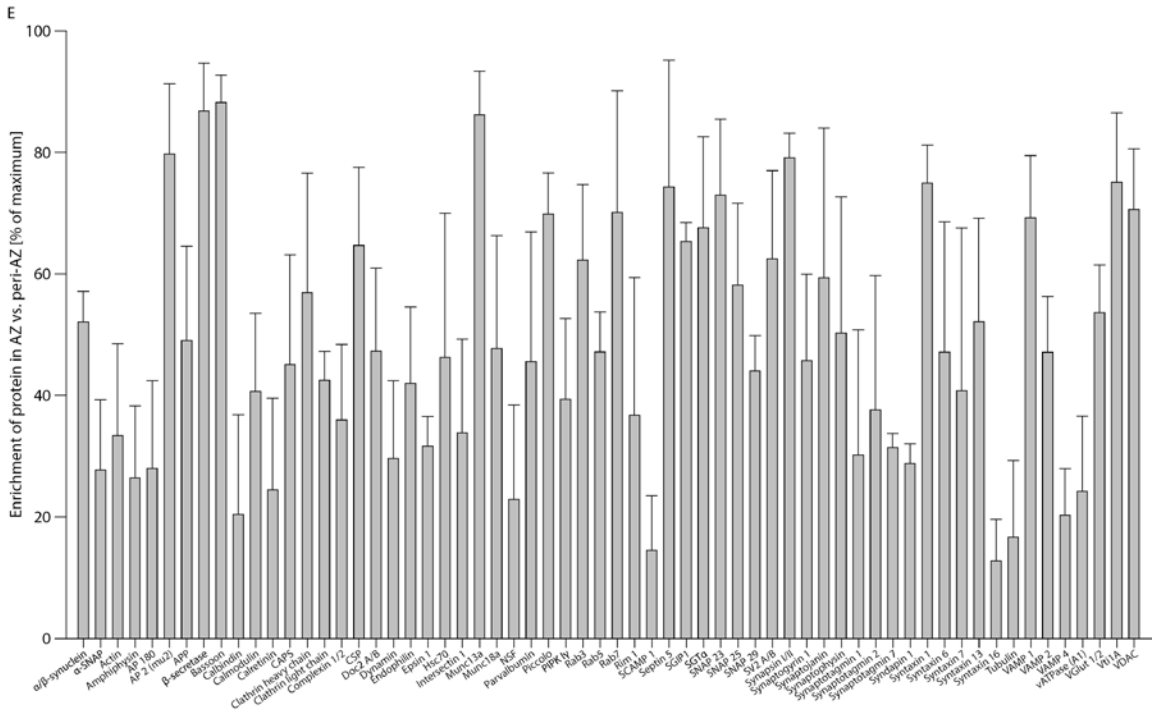
E
Enrichment of protein in AZ vs. peri-AZ [% of maximum]
100
80
60
40
20
0
α/β-synuclein
α-SNAP
Actin
Amphiphysin
AP 180
AP 2 (mu2)
APP
β-secretase
Bassoon
Calbindin
Calmodulin
Calretinin
CAPS
Clathrin heavy chain
Clathrin light chain
Complexin 1/2
CSP
Doc2 A/B
Dynamin
Endophilin
Epsin 1
Hsc70
Intersectin 1
Munc13a
Munc18a
NGF
Parvalbumin
Piccolo
PIPK Iγ
Rab3
Rab5
Rab7
Rim 1
SCAMP 1
Septin 5
SGIP 1
SGTB
SNAP 23
SNAP 25
SNAP 29
SV2 A/B
Synapsin I/II
Synaptogyrin 1
Synaptophilin
Synaptophysin
Synaptotagmin 1
Synaptotagmin 2
Synaptotagmin 7
Synaptotagmin 11
Syntaxin 1
Syntaxin 6
Syntaxin 7
Syntaxin 13
Syntaxin 16
Tubulin
VAMP 1
VAMP 2
VAMP 4
vATPase [A1]
VGlut 1/2
Vti1A
VDAC

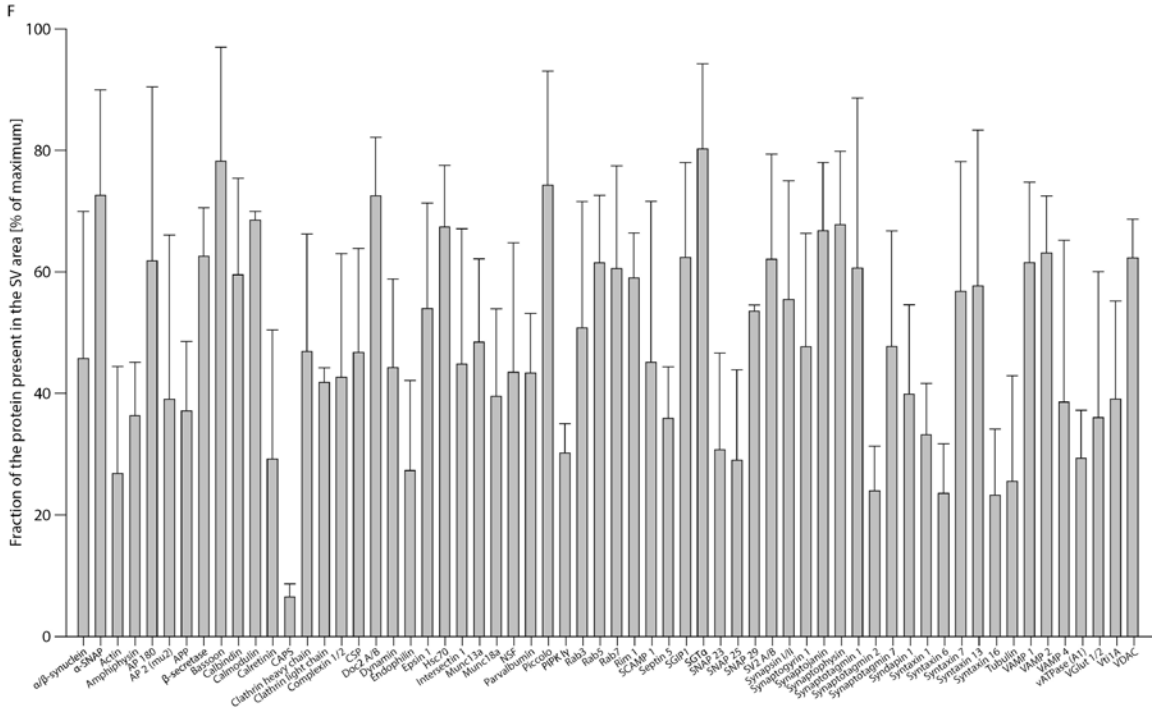
F
Fraction of the protein present in the SV area [% of maximum]
100
80
60
40
20
0
α/β-synuclein
α-SNAP
Actin
Amphiphysin
AP 180
AP 2 (mu2)
APP
β-secretase
Bassoon
Calbindin
Calmodulin
Calretinin
CAPS
Clathrin heavy chain
Clathrin light chain
Complexin 1/2
CSP
Doc2 A/B
Dynamin
Endophilin
Epsin 1
Hsc70
Intersectin 1
Munc13a
Munc18a
NGF
Parvalbumin
Piccolo
PIPK Iγ
Rab3
Rab5
Rab7
Rim 1
SCAMP 1
Septin 5
SGIP 1
SGTB
SNAP 23
SNAP 25
SNAP 29
SV2 A/B
Synapsin I/II
Synaptogyrin 1
Synaptophilin
Synaptophysin
Synaptotagmin 1
Synaptotagmin 2
Synaptotagmin 7
Syntaxin 1
Syntaxin 6
Syntaxin 7
Syntaxin 13
Syntaxin 16
Tubulin
VAMP 1
VAMP 2
VAMP 4
vATPase [A1]
VGlut 1/2
Vti1A
VDAC

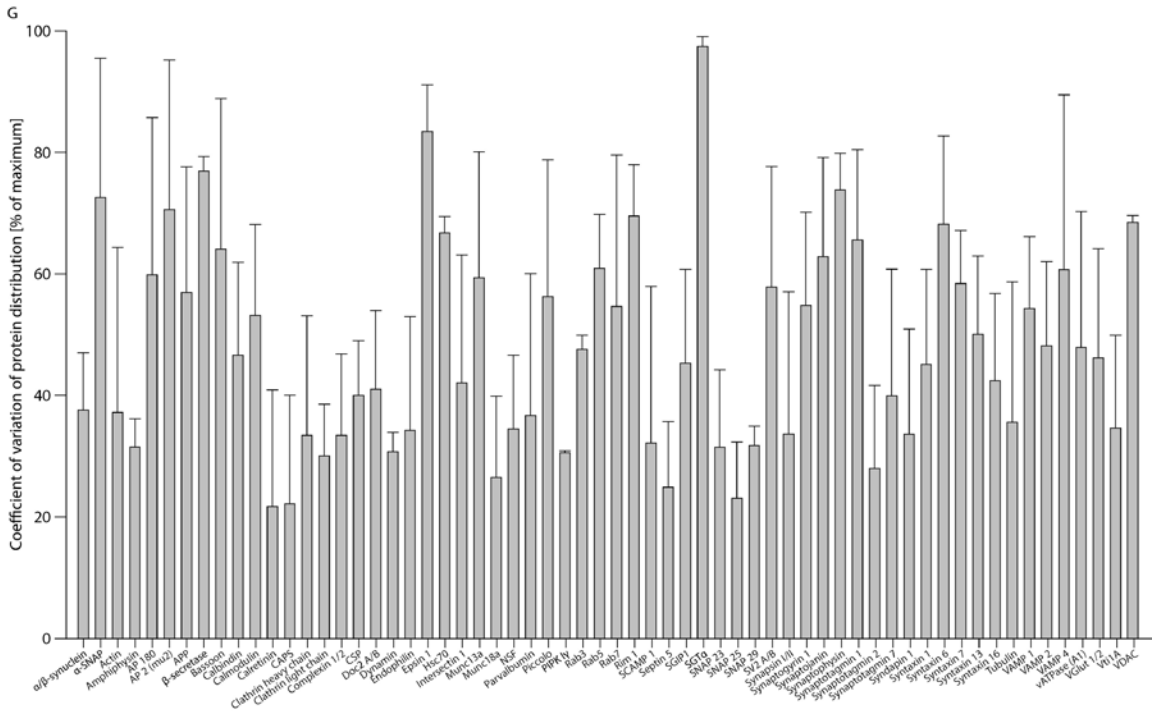
G
Coefficient of variation of protein distribution [% of maximum]
100
80
60
40
20
0
α/β-synuclein
α-SNAP
Actin
Amphiphysin
AP 180
AP 2 (mu2)
APP
β-secretase
Bassoon
Calbindin
Calmodulin
Calretinin
CAPS
Clathrin heavy chain
Clathrin light chain
Complexin 1/2
CSP
Doc2 A/B
Dynamin
Endophilin
Epsin 1
Hsc70
Intersectin 1
Munc13a
Munc18a
NGF
Parvalbumin
Piccolo
PIPK Iγ
Rab3
Rab5
Rab7
Rim 1
SCAMP 1
Septin 5
SGIP 1
SGTB
SNAP 23
SNAP 25
SNAP 29
Sv2 A/B
Synapsin I/II
Synaptogyrin 1
Synaptojanin
Synaptophysin
Synaptotagmin 1
Synaptotagmin 2
Synaptotagmin 7
Synaptotagmin 11
Synaptotagmin 12
Synaptotagmin 13
Synaptotagmin 14
Synaptotagmin 15
Synaptotagmin 16
Synaptotagmin 17
Synaptotagmin 7
Syndapin 1
Syntaxin 1
Syntaxin 6
Syntaxin 7
Syntaxin 12
Syntaxin 16
Tubulin
VAMP 1
VAMP 2
VAMP 4
vATPase [A1]
VGlut 1/2
Vti1A
VDAC

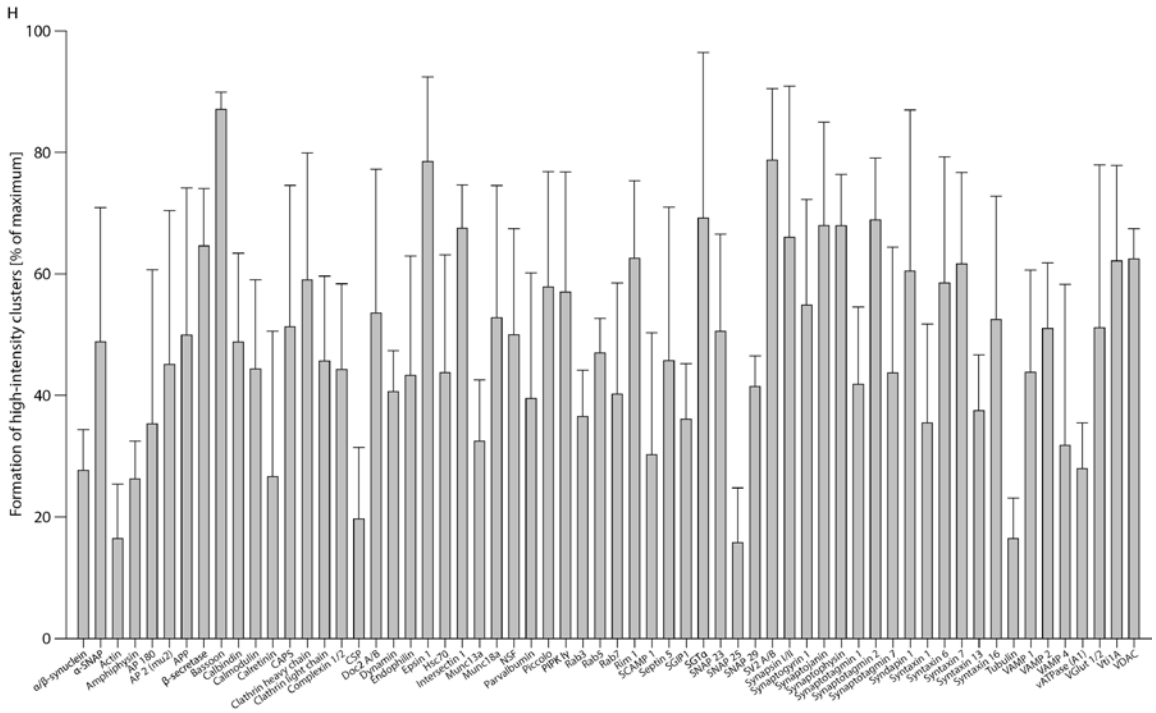
H
Formation of high-intensity clusters [% of maximum]
100
80
60
40
20
0
α/β-synuclein
α-SNAP
Actin
Amphiphysin
AP 180
AP 2 (mu2)
APP
β-secretase
Bassoon
Calbindin
Calmodulin
Calretinin
CAPS
Clathrin heavy chain
Clathrin light chain
Complexin 1/2
CSP
Doc2 A/B
Dynamin
Endophilin
Epsin 1
Hsc70
Intersectin 1
Munc13a
Munc18a
NGF
Parvalbumin
Piccolo
PIPK Iγ
Rab3
Rab5
Rab7
Rim 1
SCAMP 1
Septin 5
SGIP 1
SGTB
SNAP 23
SNAP 25
SNAP 29
Sv2 A/B
Synapsin I/II
Synaptogyrin 1
Synaptojanin
Synaptophysin
Synaptotagmin 1
Synaptotagmin 2
Synaptotagmin 7
Syndapin 1
Syntaxin 1
Syntaxin 6
Syntaxin 7
Syntaxin 12
Syntaxin 16
Tubulin
VAMP 1
VAMP 2
VAMP 4
vATPase [A1]
VGlut 1/2
Vti1A
VDAC

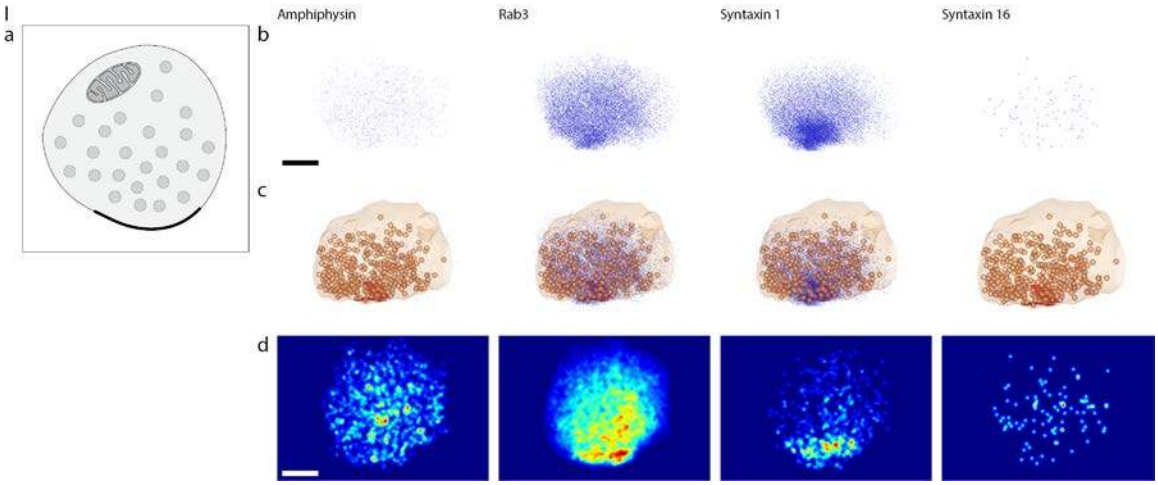

Fig. S7. Analysis of spatial parameters of different presynaptic proteins

We analyzed for each protein the following: (A) the Pearson's correlation to the active zone, defined by the bassoon immunostaining; (B) the Pearson's correlation to the vesicle cluster, defined by synaptophysin immunostaining; (C) the proportion of the protein present in the active zone area (defined as a 100-nm diameter area surrounding the bassoon signal); (D) the fraction of the protein present in the peri-active zone area (a 50-nm diameter circle surrounding the active zone area); (e) the enrichment of the protein in the active zone area, compared to the peri-active zone area (equivalent to the ratio of the previous two values); (F) the fraction of the protein present in the vesicle cluster area (defined as the area covered by the synaptophysin signal); (G) the coefficient of variation of the protein signal; (H) the fraction of the protein present in high-intensity clusters. Data are means ± SEM from the three different synaptic preparations (synaptosomes, hippocampal cultures, and neuromuscular junctions).

In panel I we used these parameters to model the distribution of amphiphysin, Rab3, syntaxin 1 and syntaxin 16 in the synaptosome we used in Fig. 5 and Fig. 6. Panel Ia indicates the preparation modeled (synaptosome). Panel Ib shows the 3D distributions of the proteins; panel Ic shows the same distributions overlapped with the synaptosome model (active zone shown in red; membranes, including synaptic vesicles, in different shades of beige). Finally, in panel Id we generated in silico fluorescence images for the four proteins (see19); note that these images correlate with the relative spatial distribution images from Fig. 4: amphiphysin is distributed throughout the synaptosome volume, Rab3 correlates with the synaptic vesicles, syntaxin 1 correlates with the active zone, while syntaxin 16 results in a low-abundance, spotty distribution. This indicates that the imaging parameters we obtained (panels A-H) can be used to model protein distributions within the synaptosome.

Additional Data Table S1 (separate file). Quantitative Western Blot measurements of presynaptic proteins

The table lists all the proteins quantified using quantitative immunoblots as outlined in Fig. 1D,E. The proteins are shown alphabetically. The table contains the functional category to which the proteins belong (2nd column), the percentage of total protein they represent (3rd column), the copy number per synapse (4th column, mean ± SEM of 4 independent preparations), and the molar concentration, calculated assuming the protein to be homogeneously distributed in the entire synaptic volume with the exception of the mitochondrial volume (5th column). Two proteins present in the synaptosome preparation, but not within the presynaptic bouton, are show in yellow, for comparison purposes.
Comments column:
[1]Synuclein. We determined the overall copy number of both α and β isoforms; the ratio between the two was 0.98:1 (α-synuclein to β-synuclein), as determined by iBAQ mass spectrometry.
[2]Protein number that was corrected assuming that the protein is also present in other particles in the sample.
[3]Protein number expected to be an underestimate, as the protein is only present in a fraction of the synapses investigated. For VGlut, which seems to be present in ~90% of the synapses we investigated21, this underestimate is relatively small. For calbindin, calretinin and parvalbumin, the underestimate is higher, since these proteins are thought to be present in at most ~5% of all synapses. Correct copy numbers for the synapses containing these proteins are therefore at least 20-fold higher.
[4]Protein numbers that were corrected for loss during purification (see Fig. S2).
[5]Epsin 1, a member of the Epsin protein family; the iBAQ mass spectrometry analysis suggests that all members of this family sum to ~500 copies per synapse.

Additional Data Table S2 (separate file). Quantitative iBAQ measurements of selected presynaptic proteins

The table lists presynaptic protein numbers determined using quantitative mass spectrometry (iBAQ). As in Table S1, we show the functional category of the protein, the number of molecules per synapse (mean ± SEM of 4 independent preparations), and the molar concentration (calculated assuming the protein to be homogeneously distributed in the entire synapse).
Comments column:
[1]Protein number expected to be an underestimate, as the protein is present only in a fraction of the synapses investigated. VGat is present in less than ~10% of the synapses investigated (*8*). Correct copy numbers for the VGat-containing synapses are therefore 10-fold higher.

Additional Data Table S3 (separate file). Database of information on the abundance of additional proteins in the preparation

The different worksheets present the abundance of different proteins in the preparation, determined using quantitative mass spectrometry (iBAQ). The proteins are listed according to the organelles in which they are thought to reside (indicated by the name of each worksheet).

For all pre-synaptic proteins, the average copy number per synaptic bouton can be calculated according to the following formula:

Average copy number = (mean% *6.0361*10^8) / (protein molecular weight)
(note that the unit of the coefficient, 6.0361*10^8, is Dalton)

For example, for tomosyn (syntaxin binding protein 5, *Stxbp5*), the 628th protein on the "Remaining" list, the mean% is 0.01984. The molecular weight of the protein is 127,659 Dalton (www.uniprot.org). The average copy number is then: (0.01984*6.0361*10^8)/127659, which is ~94 copies per synaptic bouton.

For all mitochondrial proteins, the copy numbers need to be adjusted for the known contamination of the preparation with mitochondria (Fig. S1). The resulting formula is:

Average mitochondrial protein copy number = (mean% *1.9378*10^8) / (protein molecular weight)

Movie S1. A view of presynaptic organization

The following legend is also included in the movie frames:
The synapse organization was modeled as described.
Script (indicating approximate time intervals in minutes and seconds):
00:00 to 00:12 Lateral view of the synaptic bouton. Pink-colored protein is APP. The active zone area is shown by the fire-red shading.
00:12 to 00:24 Lateral view of the synaptic bouton, with the plasma membrane transparent. Red patches are formed by SNAP 25.
00:24 to 00:37 Lateral view of the synaptic bouton, without the plasma membrane lipids and proteins. The cytosolic proteins are visible.
00:37 to 00:42 All cytosolic proteins are removed, with the exception of synapsin (light green) and cytoskeletal elements: microtubules (brick-colored), actin (purple) and septin (moss-green) are visible.
00:43 to 00:53 Synapsin is also removed, to allow a view on the organelles and cytoskeleton. The mitochondrion outer membrane is shown in cream color.
00:54 onwards: Switching to a longitudinal section through the synapse.
00:54 to 00:57 All proteins are shown.
00:58 to 01:01 Synapsin is removed, but all other proteins are shown.
01:02 to 01:05 All cytosolic proteins but cytoskeletal elements are removed.

01:06 to 01:08 All organelles are removed. Only the plasma membrane, mitochondrion outer membrane and cytoskeleton are visible.
01:09 to 01:12 The cytoskeleton is removed as well.
01:13 to 01:17 The proteins involved in cargo delivery are shown.
01:17 to 01:21 The proteins involved in the retrieval of vesicle components are shown.
01:22 to 01:29 A view of the synapse without the cytosolic proteins. The organelles and the cytoskeleton are shown. The camera zooms onto a plasma membrane area at time 01:29.
01:29 to 01:39 Same view of the synapse. The camera moves towards a microtubule and an actin microfilament.
01:39 to 01:45 Same view of the synapse. The camera moves towards a synaptic vesicle.
01:45 to 01:48 Detailed view of the synaptic vesicle. See figure 5 for the legend for the different proteins.
01:49 to 01:52 The same synaptic vesicle is shown in presence of cytosolic proteins, with the exception of synapsin.
01:52 to 01:56 Synapsin, in light green, is also added.
01:57 to 02:05 The cytosolic proteins are again removed, and the camera moves towards the active zone. The active zone proteins are shown. Prominent are Munc13 (red), bassoon (cyan), Piccolo (brown).
02:06 to 02:12 The camera moves towards a vesicle in the process of endocytosis.
02:12 to 02:16 Clathrin molecules are added above the synaptic vesicle.
02:16 to 02:24 The camera moves above the active zone. Cytosolic proteins are shown only if they are within 100 nm from the plasma membrane,
02:24 to 02:28 All cytosolic proteins are added. The view of the synapse contains now all of the elements we analyzed.
02:28 to 02:35 The camera zooms out, and shows again the synapse view containing all proteins.

References

1. V. Haucke, E. Neher, S. J. Sigrist, Protein scaffolds in the coupling of synaptic exocytosis and endocytosis. *Nat. Rev. Neurosci.* **12**, 127–138 (2011). doi:10.1038/nrn2948 Medline

2. R. Jahn, D. Fasshauer, Molecular machines governing exocytosis of synaptic vesicles. *Nature* **490**, 201–207 (2012). doi:10.1038/nature11320 Medline

3. T. C. Südhof, The synaptic vesicle cycle. *Annu. Rev. Neurosci.* **27**, 509–547 (2004). doi:10.1146/annurev.neuro.26.041002.131412 Medline

4. P. Hoopmann, A. Punge, S. V. Barysch, V. Westphal, J. Bückers, F. Opazo, I. Bethani, M. A. Lauterbach, S. W. Hell, S. O. Rizzoli, Endosomal sorting of readily releasable synaptic vesicles. *Proc. Natl. Acad. Sci. U.S.A.* **107**, 19055–19060 (2010). doi:10.1073/pnas.1007037107 Medline

5. V. Uytterhoeven, S. Kuenen, J. Kasprowicz, K. Miskiewicz, P. Verstreken, Loss of skywalker reveals synaptic endosomes as sorting stations for synaptic vesicle proteins. *Cell* **145**, 117–132 (2011). doi:10.1016/j.cell.2011.02.039 Medline

6. S. O. Rizzoli, I. Bethani, D. Zwilling, D. Wenzel, T. J. Siddiqui, D. Brandhorst, R. Jahn, Evidence for early endosome-like fusion of recently endocytosed synaptic vesicles. *Traffic* **7**, 1163–1176 (2006). doi:10.1111/j.1600-0854.2006.00466.x Medline

7. D. G. Nicholls, T. S. Sihra, Synaptosomes possess an exocytotic pool of glutamate. *Nature* **321**, 772–773 (1986). doi:10.1038/321772a0 Medline

8. S. Takamori, M. Holt, K. Stenius, E. A. Lemke, M. Grønborg, D. Riedel, H. Urlaub, S. Schenck, B. Brügger, P. Ringler, S. A. Müller, B. Rammner, F. Gräter, J. S. Hub, B. L. De Groot, G. Mieskes, Y. Moriyama, J. Klingauf, H. Grubmüller, J. Heuser, F. Wieland, R. Jahn, Molecular anatomy of a trafficking organelle. *Cell* **127**, 831–846 (2006). doi:10.1016/j.cell.2006.10.030 Medline

9. F. Opazo, A. Punge, J. Bückers, P. Hoopmann, L. Kastrup, S. W. Hell, S. O. Rizzoli, Limited intermixing of synaptic vesicle components upon vesicle recycling. *Traffic* **11**, 800–812 (2010). doi:10.1111/j.1600-0854.2010.01058.x Medline

10. M. Darna, I. Schmutz, K. Richter, S. V. Yelamanchili, G. Pendyala, M. Höltje, U. Albrecht, G. Ahnert-Hilger, Time of day-dependent sorting of the vesicular glutamate transporter to the plasma membrane. *J. Biol. Chem.* **284**, 4300–4307 (2009). doi:10.1074/jbc.M805480200 Medline

11. S. A. Mutch, P. Kensel-Hammes, J. C. Gadd, B. S. Fujimoto, R. W. Allen, P. G. Schiro, R. M. Lorenz, C. L. Kuyper, J. S. Kuo, S. M. Bajjalieh, D. T. Chiu, Protein quantification at the single vesicle level reveals that a subset of synaptic vesicle proteins are trafficked with high precision. *J. Neurosci.* **31**, 1461–1470 (2011). doi:10.1523/JNEUROSCI.3805-10.2011 Medline

12. B. Schwanhäusser, D. Busse, N. Li, G. Dittmar, J. Schuchhardt, J. Wolf, W. Chen, M. Selbach, Global quantification of mammalian gene expression control. *Nature* **473**, 337–342 (2011). doi:10.1038/nature10098 Medline

13. J. Cox, M. Mann, MaxQuant enables high peptide identification rates, individualized p.p.b.-range mass accuracies and proteome-wide protein quantification. *Nat. Biotechnol.* **26**, 1367–1372 (2008). doi:10.1038/nbt.1511 Medline

14. J. Cox, N. Neuhauser, A. Michalski, R. A. Scheltema, J. V. Olsen, M. Mann, Andromeda: A peptide search engine integrated into the MaxQuant environment. *J. Proteome Res.* **10**, 1794–1805 (2011). doi:10.1021/pr101065j Medline

15. R. Mohrmann, H. de Wit, M. Verhage, E. Neher, J. B. Sørensen, Fast vesicle fusion in living cells requires at least three SNARE complexes. *Science* **330**, 502–505 (2010). doi:10.1126/science.1193134 Medline

16. R. Sinha, S. Ahmed, R. Jahn, J. Klingauf, Two synaptobrevin molecules are sufficient for vesicle fusion in central nervous system synapses. *Proc. Natl. Acad. Sci. U.S.A.* **108**, 14318–14323 (2011). doi:10.1073/pnas.1101818108 Medline

17. G. van den Bogaart, M. G. Holt, G. Bunt, D. Riedel, F. S. Wouters, R. Jahn, One SNARE complex is sufficient for membrane fusion. *Nat. Struct. Mol. Biol.* **17**, 358–364 (2010). doi:10.1038/nsmb.1748 Medline

18. Y. Cheng, W. Boll, T. Kirchhausen, S. C. Harrison, T. Walz, Cryo-electron tomography of clathrin-coated vesicles: Structural implications for coat assembly. *J. Mol. Biol.* **365**, 892–899 (2007). doi:10.1016/j.jmb.2006.10.036 Medline

19. H. T. McMahon, E. Boucrot, Molecular mechanism and physiological functions of clathrin-mediated endocytosis. *Nat. Rev. Mol. Cell Biol.* **12**, 517–533 (2011). doi:10.1038/nrm3151 Medline

20. A. V. Shnyrova, P. V. Bashkirov, S. A. Akimov, T. J. Pucadyil, J. Zimmerberg, S. L. Schmid, V. A. Frolov, Geometric catalysis of membrane fission driven by flexible dynamin rings. *Science* **339**, 1433–1436 (2013). doi:10.1126/science.1233920 Medline

21. K. I. Willig, S. O. Rizzoli, V. Westphal, R. Jahn, S. W. Hell, STED microscopy reveals that synaptotagmin remains clustered after synaptic vesicle exocytosis. *Nature* **440**, 935–939 (2006). doi:10.1038/nature04592 Medline

22. A. Denker, I. Bethani, K. Kröhnert, C. Körber, H. Horstmann, B. G. Wilhelm, S. V. Barysch, T. Kuner, E. Neher, S. O. Rizzoli, A small pool of vesicles maintains synaptic activity in vivo. *Proc. Natl. Acad. Sci. U.S.A.* **108**, 17177–17182 (2011). doi:10.1073/pnas.1112688108 Medline

23. D. Bar-On, S. Wolter, S. van de Linde, M. Heilemann, G. Nudelman, E. Nachliel, M. Gutman, M. Sauer, U. Ashery, Super-resolution imaging reveals the internal architecture of nano-sized syntaxin clusters. *J. Biol. Chem.* **287**, 27158–27167 (2012). doi:10.1074/jbc.M112.353250 Medline

24. J. J. Sieber, K. I. Willig, R. Heintzmann, S. W. Hell, T. Lang, The SNARE motif is essential for the formation of syntaxin clusters in the plasma membrane. *Biophys. J.* **90**, 2843–2851 (2006). doi:10.1529/biophysj.105.079574 Medline

25. J. J. Sieber, K. I. Willig, C. Kutzner, C. Gerding-Reimers, B. Harke, G. Donnert, B. Rammner, C. Eggeling, S. W. Hell, H. Grubmüller, T. Lang, Anatomy and dynamics of a

supramolecular membrane protein cluster. *Science* **317**, 1072–1076 (2007). doi:10.1126/science.1141727 Medline

26. V. N. Murthy, T. Schikorski, C. F. Stevens, Y. Zhu, Inactivity produces increases in neurotransmitter release and synapse size. *Neuron* **32**, 673–682 (2001). doi:10.1016/S0896-6273(01)00500-1 Medline

27. V. Marra, J. J. Burden, J. R. Thorpe, I. T. Smith, S. L. Smith, M. Häusser, T. Branco, K. Staras, A preferentially segregated recycling vesicle pool of limited size supports neurotransmission in native central synapses. *Neuron* **76**, 579–589 (2012). doi:10.1016/j.neuron.2012.08.042 Medline

28. T. Rose, P. Schoenenberger, K. Jezek, T. G. Oertner, Developmental refinement of vesicle cycling at Schaffer collateral synapses. *Neuron* **77**, 1109–1121 (2013). doi:10.1016/j.neuron.2013.01.021 Medline

29. L. D. Cohen, R. Zuchman, O. Sorokina, A. Müller, D. C. Dieterich, J. D. Armstrong, T. Ziv, N. E. Ziv, Metabolic turnover of synaptic proteins: Kinetics, interdependencies and implications for synaptic maintenance. *PLOS ONE* **8**, e63191 (2013). doi:10.1371/journal.pone.0063191 Medline

30. D. Bonanomi, F. Benfenati, F. Valtorta, Protein sorting in the synaptic vesicle life cycle. *Prog. Neurobiol.* **80**, 177–217 (2006). doi:10.1016/j.pneurobio.2006.09.002 Medline

31. A. Denker, K. Kröhnert, J. Bückers, E. Neher, S. O. Rizzoli, The reserve pool of synaptic vesicles acts as a buffer for proteins involved in synaptic vesicle recycling. *Proc. Natl. Acad. Sci. U.S.A.* **108**, 17183–17188 (2011). doi:10.1073/pnas.1112690108 Medline

32. O. Shupliakov, The synaptic vesicle cluster: A source of endocytic proteins during neurotransmitter release. *Neuroscience* **158**, 204–210 (2009). doi:10.1016/j.neuroscience.2008.03.035 Medline

33. S. O. Rizzoli, Synaptic vesicle recycling: Steps and principles. *EMBO J.* **33**, 788–822 (2014). doi:10.1002/embj.201386357 Medline

34. N. Kitagawa, H. Mazon, A. J. R. Heck, S. Wilkens, Stoichiometry of the peripheral stalk subunits E and G of yeast V1-ATPase determined by mass spectrometry. *J. Biol. Chem.* **283**, 3329–3337 (2008). doi:10.1074/jbc.M707924200 Medline

35. G. Fischer von Mollard, B. Stahl, A. Khokhlatchev, T. C. Südhof, R. Jahn, Rab3C is a synaptic vesicle protein that dissociates from synaptic vesicles after stimulation of exocytosis. *J. Biol. Chem.* **269**, 10971–10974 (1994). Medline

36. D. Angaut-Petit, J. Molgo, A. L. Connold, L. Faille, The levator auris longus muscle of the mouse: A convenient preparation for studies of short- and long-term presynaptic effects of drugs or toxins. *Neurosci. Lett.* **82**, 83–88 (1987). doi:10.1016/0304-3940(87)90175-3 Medline

37. H. Schägger, Tricine-SDS-PAGE. *Nat. Protoc.* **1**, 16–22 (2006). doi:10.1038/nprot.2006.4 Medline

38. I. Bethani, T. Lang, U. Geumann, J. J. Sieber, R. Jahn, S. O. Rizzoli, The specificity of SNARE pairing in biological membranes is mediated by both proof-reading and spatial segregation. *EMBO J.* **26**, 3981–3992 (2007). doi:10.1038/sj.emboj.7601820 Medline

39. A. Pechstein, O. Shupliakov, V. Haucke, Intersectin 1: A versatile actor in the synaptic vesicle cycle. *Biochem. Soc. Trans.* **38**, 181–186 (2010). doi:10.1042/BST0380181 Medline

40. L. von Kleist, W. Stahlschmidt, H. Bulut, K. Gromova, D. Puchkov, M. J. Robertson, K. A. MacGregor, N. Tomilin, A. Pechstein, N. Chau, M. Chircop, J. Sakoff, J. P. von Kries, W. Saenger, H. G. Kräusslich, O. Shupliakov, P. J. Robinson, A. McCluskey, V. Haucke, Role of the clathrin terminal domain in regulating coated pit dynamics revealed by small molecule inhibition. *Cell* **146**, 471–484 (2011). doi:10.1016/j.cell.2011.06.025 Medline

41. K. Vervaeke, A. Lorincz, P. Gleeson, M. Farinella, Z. Nusser, R. A. Silver, Rapid desynchronization of an electrically coupled interneuron network with sparse excitatory synaptic input. *Neuron* **67**, 435–451 (2010). doi:10.1016/j.neuron.2010.06.028 Medline

42. J. Rappsilber, M. Mann, Analysis of the topology of protein complexes using cross-linking and mass spectrometry. *Cold Spring Harbor Protocols* **2007**, pdb.prot4594 (2007). doi:10.1101/pdb.prot4594 Medline

43. J. V. Olsen, L. M. de Godoy, G. Li, B. Macek, P. Mortensen, R. Pesch, A. Makarov, O. Lange, S. Horning, M. Mann, Parts per million mass accuracy on an Orbitrap mass spectrometer via lock mass injection into a C-trap. *Mol. Cell. Proteomics* **4**, 2010–2021 (2005). doi:10.1074/mcp.T500030-MCP200 Medline

44. W. Huang, B. T. Sherman, R. A. Lempicki, Bioinformatics enrichment tools: Paths toward the comprehensive functional analysis of large gene lists. *Nucleic Acids Res.* **37**, 1–13 (2009). doi:10.1093/nar/gkn923 Medline

45. W. Huang, B. T. Sherman, R. A. Lempicki, Systematic and integrative analysis of large gene lists using DAVID bioinformatics resources. *Nat. Protoc.* **4**, 44–57 (2009). doi:10.1038/nprot.2008.211 Medline

46. T. Staudt, M. C. Lang, R. Medda, J. Engelhardt, S. W. Hell, 2,2′-thiodiethanol: A new water soluble mounting medium for high resolution optical microscopy. *Microsc. Res. Tech.* **70**, 1–9 (2007). doi:10.1002/jemt.20396 Medline